Improved Modeling of Geomagnetically Induced Currents Utilizing Derivation Techniques for Substation Grounding Resistance

Maryam Kazerooni, *Student Member, IEEE*, Hao Zhu, *Member, IEEE*, and Thomas J. Overbye, *Fellow, IEEE*

Abstract—**This paper focuses on estimating the substation grounding resistance to improve the modeling of geomagnetically induced currents (GICs). Grounding resistances are not included in the standard power flow models, and their approximate values are often used for performing GIC studies. This paper provides an algorithm to estimate the resistances from the GIC measurements. This algorithm calculates the linear sensitivity factors of the GICs around the local grounding resistive components and uses linear regression to solve for the resistances. The effectiveness of the proposed algorithm is demonstrated using both a small test case as well as a 62 500-bus model of the North American Eastern Interconnection.**

Index Terms—**Geomagnetic disturbance (GMD), geomagnetically induced currents (GICs), model validation, substation grounding resistance.**

I. INTRODUCTION

SOLAR coronal holes and coronal mass ejections can disturb the Earth's geomagnetic field. These geomagnetic disturbances (GMD) in turn induce electric fields which drive low frequency currents in the transmission lines. These geomagnetically induced currents (GICs) can cause increased harmonic currents and reactive power losses by causing transformers half-cycle saturation. This may cause voltage instability by a combination of two means. First, the increased transformer reactive power losses may lead directly to voltage instability. Second, the harmonic currents might cause relay misoperation and unintended disconnection of the reactive power providers such as static VAR compensators (SVCs) [1], [2].

It has been shown that the transformer GIC is linearly related to the electric field (E-field), where the linear coefficients depend on the given power system parameters. A variety of GIC power flow software and a benchmark test case have also been developed [3]–[7].

A key factor in the GIC modeling is to calculate the linear coefficients. Because of the dc nature of GIC flows, these coefficients depends on the network topology and resistances, where the accuracy of the latter depends on the available network information. Most of the parameters required for calculating the linear coefficients are part of the standard power flow models and are usually available. The only piece of information which may not be available, but strongly affects the modeling accuracy is the substation grounding resistance. Substation grounding resistance is the effective grounding resistance of the substation neutral which includes the grounding grid and the emanating ground paths due to shield wires grounding. This parameter depends on the local soil humidity and the ground conditions. Hence, it is very challenging to obtain an accurate value for this parameter in practice.

The effect of inacurate substation grounding resistance on GIC calculations has been studied previously in literature. Reference [8] provides a mathematical technique for calculating the effect of grounding resistance on the GICs and [9] demonstrates the impacts through numerical results on the Finish 400 kV grid. In reference [11], a sensitivity analysis has been performed on the 62,500 bus Eastern Interconnection system which demonstrates the significance of grounding resistance for calculating the GIC flows. These previous papers emphasize the need to have accurate grounding resistances for GIC analysis.

A variety of techniques are available in the literature to measure the substation grounding resistance [12], [13]. Four-point method and fall-of-potential method are common procedures for measuring the earth resistivity [14]. The grounding resistance can be calculated from the resistivity through a uniform soil model where the resistivity is assumed to be the same at all depths [15]. Alternatively, a two-layered model may be used, especially at locations near lakes, rivers or mountains where the soil resistivity is not uniform in horizontal direction [16].

This paper proposes to estimate the substation grounding resistance using GIC measurements. In this technique, the GICs at the substations being tested are collected and the sensitivity of the GICs to the grounding resistances are calculated. Then, the problem is formulated in the form of linear regression model with unknown grounding resistances. By observing the GICs, the calculated sensitivity factors would become the constant coefficients of the linear model. This technique requires only the GIC measurements at the substations being tested and the information on the network topology and other system resistance

parameters. This information is part of the power flow model and is usually available with good accuracy. The effectiveness of the proposed technique is demonstrated using both a small 20 bus test case as well as a 62,500 bus model of the Eastern Interconnection (EI).

The paper is organized as follow: The GIC model is introduced in Section II. The algorithm for estimating the substation grounding resistance through GIC measurements is presented in Section III. In Section IV, the dependency of the proposed technique to the E-field is identified and proper adjustments are considered to eliminate such dependencies. Section V demonstrates the proposed technique using a 20-bus test case, while the application on a large 62500-bus system is given in Section VI. Section VII presents a conclusion and directions for future work.

II. GIC MODELING

To calculate the voltage potential induced on the transmission line, the E-field is integrated over the length of the line. Assuming a uniform E-field, the DC voltage on the line between bus n and m is expressed in:

$$V_{nm} = e^N L_{nm}^N + e^E L_{nm}^E \qquad (1)$$

where L_{nm}^N and L_{nm}^E denote the northward and eastward line distances; and e^N and e^E are the northward and eastward E-fields, respectively. The induced voltages are converted to the dc current injections through Norton Equivalent, and the total current injections are derived from Kirchhoffs current law (KCL) [3]. The vector of current injections is obtained by putting all the current injections together as given by $I^{Nor} = \mathbf{C}E$ where $\mathbf{C}$ depends on the length, orientation and resistance of the lines.

KCL is used to write the nodal network equations and obtain the bus voltages from the current injections as given by

$$\mathbf{V} = \mathbf{G}^{-1} I^{Nor} \qquad (2)$$

where matrix $\mathbf{G}$ is similar to the bus admittance matrix except that it only captures the conductance values and is modified to include substation groundings. By Ohm's law, the GICs are related to the bus voltages:

$$I = \mathbf{G}^S \mathbf{V} = (\mathbf{G}^S \mathbf{G}^{-1}) I^{Nor} = (\mathbf{G}^S \mathbf{G}^{-1} \mathbf{C})E = \mathbf{H}E \quad (3)$$

where I is the vector of transformers neutral currents, E is the E-field vector, $\mathbf{G}^S$ is a diagonal matrix with the grounding resistances on its diagonal and $\mathbf{H}$ is the coefficient matrix defined as $\mathbf{H} := \mathbf{G}^S \mathbf{G}^{-1} \mathbf{C}$. This model indicates that the GICs are linearly dependent on the E-field though the coefficient matrix $\mathbf{H}$. Matrix $\mathbf{H}$ only depends on the network topology and resistances. Most of this information is part of the standard power flow model and is known with reasonable accuracy. The line resistances depend on the temperature which could introduce uncertainty. However, the amount of their variation with temperature is known (0.4% per degree Celsius) and therefore, the uncertainty can be excluded by incorporating approximate temperature profiles in the model [10]. Substation grounding resistance is the only piece of information which is often unknown and is approximated with a large degree of uncertainty.

At each instant in time, the E-field has two components: the eastward field e^E and the northward field e^N. Hence, the GIC

model can be rewritten as:

$$I = [H^E \mid H^N] \times \begin{bmatrix} e^E \\ e^N \end{bmatrix} \qquad (4)$$

where H^E and H^N are the eastward and northward coefficients.

The GIC model represents the whole electrical network and the GIC vector I includes the neutral currents of all the transformers. For a large system, the whole network is not of interest, and it is desired to reduce the model to cover only specific transformers. This can be done by selecting only the corresponding entries in the I matrix and truncating the coefficient matrix accordingly.

A. Matrix Form of the GIC Model

During the GMD, the E-field is dynamic over the discrete time horizon $\mathcal{T} := \{t^1, t^2, ..., t^T\}$, which can be concatenated into the $2 \times T$ matrix:

$$\mathbf{E} = \begin{bmatrix} e^{E,t^1} & e^{E,t^2} & \cdots & e^{E,t^T} \\ e^{N,t^1} & e^{N,t^2} & \cdots & e^{N,t^T} \end{bmatrix} = \begin{bmatrix} E^E \\ E^N \end{bmatrix} \qquad (5)$$

where e^{E,t^n} and e^{N,t^n} are respectively, the eastward and northward E-fields at the nth time instant; and E^E and E^N are the E-field time series in east and north direction, respectively. Similarly, for the dynamic GIC flow I to form the matrix:

$$\mathbf{Y} = \begin{bmatrix} z_1^{t^1} & z_1^{t^2} & \cdots & z_1^{t^T} \\ z_2^{t^1} & z_2^{t^2} & \cdots & z_2^{t^T} \\ \vdots & \vdots & \ddots & \vdots \\ z_K^{t^1} & z_K^{t^2} & \cdots & z_K^{t^T} \end{bmatrix} \qquad (6)$$

where $z_k^{t^n}$ is the GIC reading of the kth sensor at the nth time instant and K is the total number of sensors. The GIC sensors are installed at the transformers neutral and measure the DC current passing through its neutral. The matrix form of the linear GIC model is given by

$$\mathbf{Y} = \mathbf{H}\mathbf{E} + \mathbf{N} \qquad (7)$$

where $\mathbf{N}$ is the measurement noise.

III. GROUNDING RESISTANCE ESTIMATION

The grounding resistance error is described as the vector of the differences between the actual grounding resistances and the assumed ones as given by

$$\partial R = R - R_0 \qquad (8)$$

where R is the vector containing the actual grounding resistance of all the substations and R_0 is the vector of the assumed grounding resistances.

The sensitivity of the GIC to the grounding resistance is defined as the percent variation of the current in terms of the percent variation of the grounding resistance as given by [11]:

$$s_{ij} = \frac{\partial(\% I_{GIC,i})}{\partial(\% R_j)} = \frac{(\partial I_{GIC,i}/I_{GIC,i})}{(\partial R_j/R_j)}. \qquad (9)$$

In this paper, the actual variation is used instead of the percent variation to simplify the problem formulation: $s_{ij} =$

Algorithm 1: Grounding Resistance Estimation with E-field.

t

1:   **procedure**   GROUNDING RESISTANCE ESTIMATION WITH E-FIELD ($\mathbf{Y}$, $\mathbf{X}$, R_0)

2:     Initialize the estimated resistances $\hat{R}$ to R_0

3:     Define the convergence tolerance, ε

4:     Initialize ∂R to the all-ones vector

5:     **while** $|\partial R| > \varepsilon$ **do**

6:       Calculate the sensitivities $\mathbf{S}^N$ and $\mathbf{S}^E$

7:       Calculate $\mathbf{Y}_b = \mathbf{H}\mathbf{E}$

8:       Calculate $\mathbf{A} = (E^E \otimes \mathbf{S}^E + E^N \otimes \mathbf{S}^N)^T$

9:       Solve for ∂R through
$\partial R = (\mathbf{A}^T\mathbf{A})^{-1}\mathbf{A}^T vec(\mathbf{Y} - \mathbf{Y}_b)$

10:     Update the resistances by $\hat{R} = \hat{R} + \partial R$

11:     **end while**

12:     **return** $\hat{R}$

13:   **end procedure**

Algorithm 2: Sensitivity Calculation.

1:   **procedure** SENSITIVITY CALCULATION (R)

2:     Initialize the grounding resistances to R

3:     Enforce an eastward E-field to get I^{E0}.

4:     Enforce a northward E-field to get I^{N0}.

5:     **for** $n = 1$ to $n < \text{K}$ **do**

6:       Increase the resistance of substation n by 10%.

7:       Enforce an eastward E-field to get I^E.

8:       Enforce a northward E-field to get I^N.

9:       Calculate the nth column of the northward sensitivity matrix by $S_n^E = 10(I^E - I^{E0})/I^{E0}$

10:      Calculate the nth column of the northward sensitivity matrix by $S_n^N = 10(I^N - I^{N0})/I^{N0}$

11:      Set the resistance of substation n back to default.

12:     **end for**

13:     **return** $\mathbf{S}^N$ and $\mathbf{S}^E$

14:   **end procedure**

$\partial I_{GIC,i}/\partial R_j$. For a set of K substations, one can build the $K \times K$ sensitivity matrix $S = \{s_{ij}\}$ where s_{ij} is the sensitivity of the GIC at substation i to the grounding resistance of substation j. The sensitivity depends on the E-field direction and the sensitivity matrix is defined for a particular direction. Let $\mathbf{S}^N$ and $\mathbf{S}^E$ denote the sensitivity matrices for northward and eastward E-fields. The grounding resistance error modifies the coefficient matrix by

$$\begin{cases} H^N \leftarrow H^N + \mathbf{S}^N \partial R \\ H^E \leftarrow H^E + \mathbf{S}^E \partial R \end{cases}. \qquad (10)$$

Substituting the updated coefficient matrix in the GIC model gives rise to

$$[(H^N + \mathbf{S}^N \partial R) \mid (H^E + \mathbf{S}^E \partial R)] \times \mathbf{E} = \mathbf{Y}. \qquad (11)$$

Defining the matrix $\mathbf{Y}_b := \mathbf{H}\mathbf{E}$, equation (11) can be rewritten as:

$$(E^E \otimes \mathbf{S}^E + E^N \otimes \mathbf{S}^N)^T \partial R = vec(\mathbf{Y} - \mathbf{Y}_b) \qquad (12)$$

where $\otimes$ is the Kronecker product and $vec()$ is the vectorization function. Defining the matrix $\mathbf{A} := (E^E \otimes \mathbf{S}^E + E^N \otimes \mathbf{S}^N)^T$ generates an overdetermined system with ∂R as the unknown:

$$\mathbf{A}\partial R = vec(\mathbf{Y} - \mathbf{Y}_b) \qquad (13)$$

Least squares estimation can be used to estimate ∂R as given by

$$\hat{\partial R}^{LS} := \arg\min_{\partial R} \|vec(\mathbf{Y} - \mathbf{Y}_b) - \mathbf{A}\partial R\|_2$$

$$= (\mathbf{A}^T\mathbf{A})^{-1}\mathbf{A}^T vec(\mathbf{Y} - \mathbf{Y}_b). \qquad (14)$$

The coefficients modification presented in (10) is valid only for small values of ∂R as the sensitivities are linear approximations. However, ∂R may be large when the grounding resistance data is inaccurate or unavailable. To tackle this, the process can be performed iteratively until ∂R converges to zero. The resistances obtained at each iteration are used as the initial values for the consecutive iteration. The steps of this iterative algorithm are described in Algorithm 1.

The inputs of the algorithm are the GIC measurements $\mathbf{Y}$, the E-field $\mathbf{E}$ and the available grounding resistances R_0. If no resistance data is available, R_0 is represented by a vector of random values within the range of 0.05 and 0.3 (reasonable range for the grounding resistance). The output of the algorithm is $\hat{R}$ which is the vector of estimated grounding resistances.

In theory, the estimated resistance obtained from the proposed technique is the same as the one measured by the conventional methods. The proposed algorithm serves as an alternative solution when measuring the resistances is not feasible for practical reasons. There are several challenges associated with the measurement-based approaches. First, external objects such as water pipelines and adjacent railroad tracks distort the earth potential contours. Second, sources of dc current such as dc railroad tracks, pipelines cathodic protection systems and dc transmission lines produce stray currents which interfere with the grounding resistance measurements. Third, the resistance of the electrodes used for the measurements can introduce error if the substation being tested has low resistivity. Last, the grounding resistance mostly depends on the humidity, salt level or temperature and therefore is time-variant and may change significantly with seasons. The conventional grounding resistance measurements are usually performed every five to ten years and even the most recent one might not capture the current state of the soil regarding its humidity, salt level or temperature. In contrast, the estimate from the GIC measurements is in semi-real time. Motivated by the negative impacts of GMDs, electric utilities are investing in the GIC monitoring enhancement. More GIC sensors are being installed in the grid which widens the applications of the proposed technique.

A. Sensitivity Calculation

The algorithm presented earlier requires calculation of the sensitivity matrices at each iteration. There are analytical techniques to derive the sensitivities as functions of the network parameters [11]. Alternatively, one can follow the sensitiv-

ity definition to calculate the sensitivities as described in Algorithm 2. The algorithm takes the grounding resistances as input. This allows calculating the sensitivities in each iteration after the grounding resistances are updated.

IV. DEPENDENCY ON THE ELECTRIC FIELD

The problem with the proposed technique is that it depends on the E-field whereas only the GIC data is assumed to be available, not the E-field. To address this issue, first, the E-field is estimated through the GICs and then is used in the algorithm. Since the grounding resistances are not available in the beginning and are going to be estimated later, a meaningful E-field estimation should be robust to the grounding resistance error. The Appendix demonstrates that the ordinary LS method can successfully estimate the E-field up to scaling even when the grounding resistances are inaccurate:

$$\hat{\mathbf{E}}^{LS} := \arg\min_{\mathbf{E}} \|\mathbf{Y} - \mathbf{H}\mathbf{E}\|_2 = (\mathbf{H}^T\mathbf{H})^{-1}\mathbf{H}^T\mathbf{Y}. \quad (15)$$

This estimation scales with the actual E-field, but the ratio is unknown. This uncertainty is included in the model through:

$$\mathbf{E} = \alpha\hat{\mathbf{E}} \Rightarrow \alpha\, vec(\hat{\mathbf{Y}}_b) + \mathbf{A}\partial R = vec(\mathbf{Y}) \quad (16)$$

where α is the unknown ratio between the estimated E-field and the actual one. $\hat{\mathbf{Y}}_b$ is similar to $\mathbf{Y}_b$ expect that the estimated E-field is used in its definition instead of the actual one: $\hat{\mathbf{Y}}_b = \mathbf{H}\hat{\mathbf{E}}$. The system is augmented to include α as an additional unknown:

$$[\mathbf{A} \mid vec(\hat{\mathbf{Y}}_b)] \times \begin{bmatrix} \partial R \\ \alpha \end{bmatrix} = vec(\mathbf{Y}). \quad (17)$$

Defining $\mathbf{x}_a := [\partial R \mid \alpha]^T$ as the augmented state and $\mathbf{A}_a := [\mathbf{A} \mid vec(\hat{\mathbf{Y}}_b)]$ as the augmented design matrix, least squares can be used to solve for ∂R and α as given by

$$\hat{x}_a^{LS} : = \arg\min_{\mathbf{x}_a} \|vec(\mathbf{Y}) - \mathbf{A}_a\mathbf{x}_a\|_2$$
$$= (\mathbf{A}_a^T\mathbf{A}_a)^{-1}\mathbf{A}_a^T vec(\mathbf{Y}). \quad (18)$$

Least squares provides the solution with the minimum Euclidean norm. However, it is better to minimize the Euclidean norm of ∂R, but allow α to take any value. To find the solution with this particular property, regularized least squares may be used as described in the following.

A. Regularized Least Squares

Ordinary least squares is the standard approach to solve the overdetermined system of equation

$$\mathbf{M}\mathbf{x} = b \quad (19)$$

where the sum of the squared residuals $\|\mathbf{M}x - b\|_2$ is minimized. Regularized least squares give preference to a particular solution with desirable properties by adding the regularization term as expressed by

$$\hat{x} := \arg\min_{\mathbf{x}} \|\mathbf{M}x - b\|_2 + \mu\|\mathbf{F}\mathbf{x}\|_2 \quad (20)$$

where $\mathbf{F}$ is suitably chosen to capture the desired regularization and μ is the penalty weight [17]. This forms a multi-objective
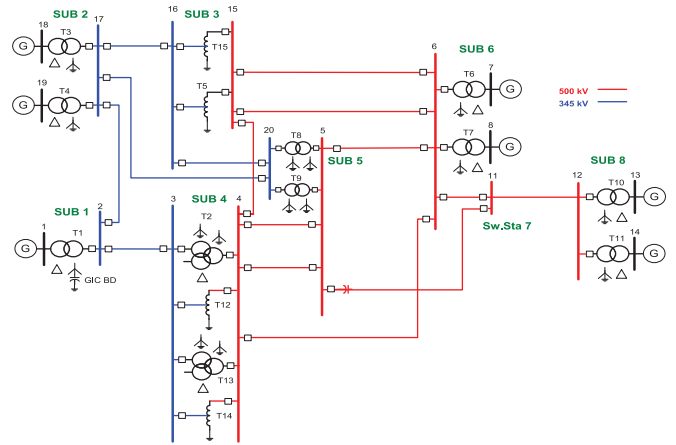

Fig. 1. Single-line diagram of the 20-bus test case in [7].

optimization problem and its closed-form solution is given by

$$\hat{x} = (\mathbf{M}^T\mathbf{M} + \mu\mathbf{F}^T\mathbf{F})^{-1}\mathbf{M}^T b. \quad (21)$$

For the augmented system in (17), it is desired to enforce ∂R to zero, but leave α unconstrained. This can be done by selecting $\mathbf{F}$ as a diagonal matrix with 1 on all its diagonal entries but the last one as given by

$$\mathbf{F} = diag([\vec{\mathbf{1}}_{(1,K)}, 0]) \quad (22)$$

where K is the number of substations. The algorithm for estimating the grounding resistance when the E-field is not available is summarized in the following:

Algorithm 3: Grounding Resistance Estimation without E-field.

1:    **procedure** GROUNDING RESISTANCE ESTIMATION WITHOUT E-FIELD ($\mathbf{Y}, R_0$)
2:      Initialize the grounding resistances $\hat{R}$ to R_0
3:      Estimate the E-field by $\hat{\mathbf{E}} = (\mathbf{H}^T\mathbf{H})^{-1}\mathbf{H}^T\mathbf{Y}$
4:      Define the convergence tolerance, ε
5:      Initialize ∂R to the all-ones vector
6:      **while** $|\partial R| > \varepsilon$ **do**
7:        Calculate the sensitivities $\mathbf{S}^N$ and $\mathbf{S}^E$
8:        Calculate $\hat{\mathbf{Y}}_b := \mathbf{H}\hat{\mathbf{E}}$
9:        Calculate
     $\mathbf{A}_a := [(E^E \otimes \mathbf{S}^E + E^N \otimes \mathbf{S}^N)^T \mid vec(\hat{\mathbf{Y}}_b)]$
10:     Solve for ∂R by
     $[\partial R \mid \alpha]^T = (\mathbf{A}_a^T\mathbf{A}_a)^{-1}\mathbf{A}_a^T vec(\mathbf{Y})$
11:     Update the resistances by $\hat{R} = \hat{R} + \partial R$
12:     **end While**
13:     **return** $\hat{R}$
14: **end procedure**

V. NUMERICAL RESULTS USING A SMALL TEST CASE

The effectiveness of the proposed method is validated though simulation. The 20-bus system in [7] is investigated with the one-line diagram shown in Fig. 1. The substation grounding resistances are presented in Table I. These values are not available to the algorithm and need to be estimated. Instead, the assumed resistances listed in the table are provided. The assumed

TABLE I
GROUNDING RESISTANCES OF THE 20-BUS TEST CASE

Name	Actual Resistance	Assumed Resistance	Error (%)
SUB1	0.20	0.31	53.53
SUB2	0.20	0.14	31.21
SUB3	0.20	0.26	27.72
SUB4	1.00	0.90	9.56
SUB5	0.10	0.03	70.00
SUB6	0.10	0.17	72.83
SUB7	0.10	0.16	61.87

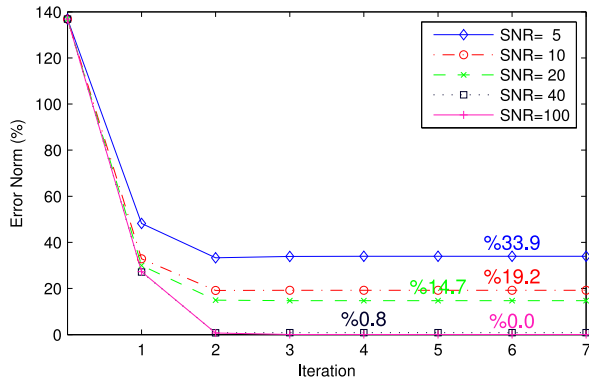Fig. 2. The estimation error for the test case when the E-field is known.

Fig. 3. The estimation error for the test case when the E-field is unknown.

grounding resistances have an average of 136% absolute error with the error defined as

$$\mathbf{Error}^{R_g} = \frac{\|R_0 - R\|_2}{\|R\|_2} \qquad (23)$$

Synthetic GIC data is created by enforcing an E-field to the system and obtaining the induced GICs through solving the GIC flow in PowerWorld Simulator. For the purpose of this paper, the E-field measured during an actual geomagnetic storm is used to maximize the alikeness with real GIC measurements [18]. The E-field collected at Fredericksburg observatory during the March 9th, 2012 storm is investigated. Fredericksburg observatory is located in the US at a latitude/longitude of 38.205°N, 77.373°W. To simulate the system perturbation and measurement noise, white Gaussian noise with different signal-noise-ratios (SNR) is added to the ideal GICs and the synthetic measurements are obtained.

First, the substation grounding resistances are estimated assuming the E-field is known using Algorithm 1. Fig. 2 illustrates the estimation error when the GIC measurements are subject to different levels of Gaussian noise. It is observed that the algorithm converges after two iterations for all the noise levels. The final estimation error which is obtained after convergence depends on the noise level, i.e. higher noise level results in higher estimation error. For example, the estimation error is 33.9% when the SNR is 5 dB and zero when SNR is 100 dB (almost noise-free).

Sometimes, the E-field is not provided to the algorithm and only the GICs are available. In this case, the algorithm first estimates the E-field based on the GICs and then uses this estimation to find the resistances as presented in Algorithm 3. This
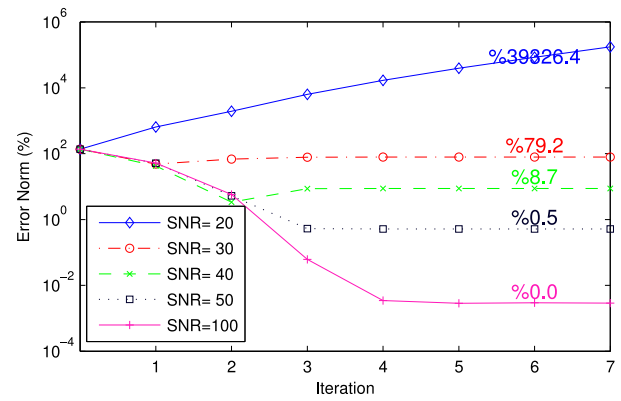
technique is implemented for different measurements noise levels as illustrated in Fig. 3. The y-axis in the figure has a logarithmic scale. It is observed that the algorithm diverges when the SNR is 20 dB or lower (higher noise level). For the SNR equal to 30 dB, the algorithm converges, but the estimation accuracy is not much improved from the initial guess; 136.9% error in the initial guess is reduced only to 79.2% which is still too high. The estimation error drops significantly for lower noise levels with the estimation error equal to 8.7%, 0.5% and zero for SNRs equal to 40 dB, 50 dB and 100 dB, respectively. Comparing these results with the ones from Fig. 2, one can conclude that the algorithm is more robust to measurements noise when the E-field is available. Moreover, the algorithm has a faster convergence rate when the E-field is available as it converges in only two iterations with the E-field as opposed to in three to four iterations without the E-field.

In practice, the GICs at all the substations are not available and only few substations have GIC sensors installed at their transformer neutrals. Hence, it is desired to evaluate the algorithm when the GIC data is sparse. To model this, only the GICs at substation 1, 2, and 3 are provided to the algorithm and the rest are unknown. In this case, the algorithm reduces the GIC model to include only the substations with available data and ignores the rest of the network. Using the reduced model, the algorithm performs similar to the normal case, but finds only the resistance of the substations included in the model. First, the substations are estimated assuming the E-field is known as illustrated in Fig. 4. For all noise levels, the error decreases after each iteration until it converges to around 10% at the third iteration. The interesting observation is that the algorithm is extremely robust to the measurement noise under this scenario and the curves for different noise levels are almost aligned. The other observation is that unlike the previous cases, the estimation error does not converge to zero when the measurements are noise-free. This is because some of the substations have inaccurate grounding resistances and yet no GIC sensors which makes it impossible to track down the error they introduce to the estimation and makes the system unobservable. Simulation results indicate that the estimation error reduces to zero when the grounding resistance of the substations that are missing GIC sensors are accurate and the GIC measurements are noise free.
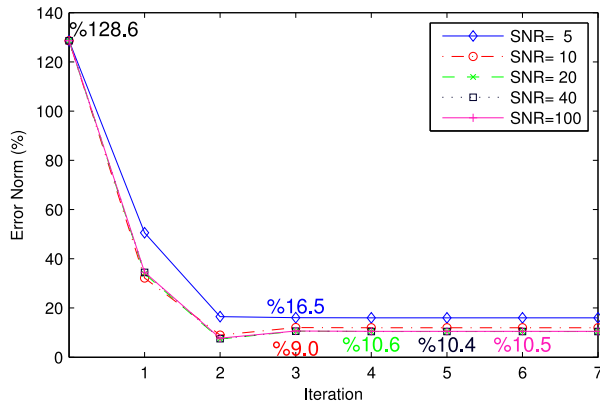
Fig. 4. The estimation error for the test case when the E-field is known and the GIC data is sparse.

Fig. 5. The estimation error for the test case when the E-field is unknown and the GIC data is sparse.

TABLE II
THE ESTIMATED RESISTANCES FOR THE TEST CASE WHEN THE GIC DATA IS SPARSE

Name	R	R_0	Initial Error (%)	$\hat{R}$	Estimation Error (%)
SUB1	0.20	0.36	81.15	0.19	4.41
SUB2	0.20	0.24	18.86	0.20	2.32
SUB3	0.20	0.40	97.91	0.22	9.28

Fig. 6. The estimation error when the assumed grounding resistances have different levels of accuracy.

The more substations with missing GIC sensors are in the system and the more inaccurate their assumed grounding resistance are, the higher the estimation error will be as verified through simulation.

It is important to realize that even though the algorithm may not provide 100% accuracy all the time, its estimation is remarkably better than the initial values. In other words, the algorithm does not find the actual resistances, but it moves towards them and converges to somewhere in their close proximity. This is demonstrated in Table II by comparing the actual resistances with the estimated ones when the GIC measurements are noise free. For reference, the initial grounding resistances are presented as well.

The next validation test is to study the performance of the algorithm when the E-field is not available and the GIC data is sparse. The GICs at the first three substations (1, 2 and 3) are provided, but the E-field and the rest of GICs are missing. The algorithm excludes the substations with missing GICs from the model, estimates the E-field from the available GICs with one level of ambiguity and finally uses regularized least squares to find the resistances. Fig. 5 illustrates the estimation error under this scenario for different measurement noise levels. The algorithm diverges when the SNR is 10 dB or lower. The algorithm converges for lower noise levels with the estimation error equal to 22.9%, 17.4% and 17.8% for SNRs equal to 10, 40 and 100, respectively. Similar to the case with the sparse GIC data and known E-field (Fig. 4), the estimation error does not reach zero when the GIC measurements are noise free. Again, this is due to the error in the grounding resistance of the substations that are missing GIC sensors and the lack of observability in these
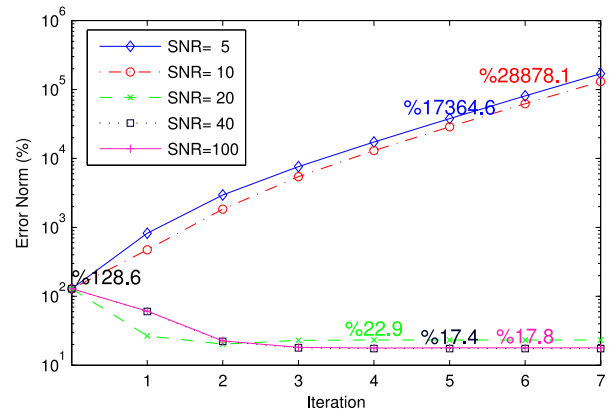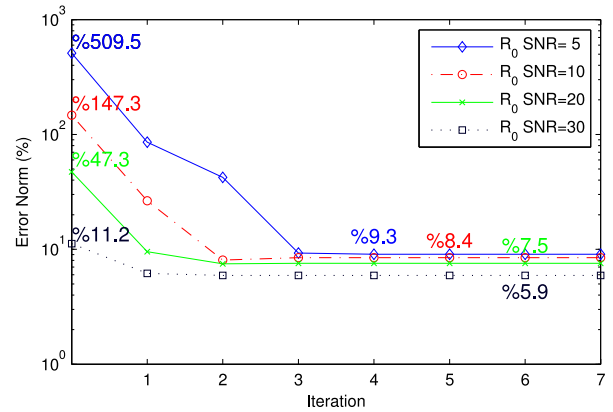
substations. If the actual grounding resistance of such substations are provided to the algorithm, the estimation error will reduce to zero in the absence of measurement noise.

Next, the effect of the assumed grounding resistances on the performance of the algorithm is studied. Four sets of assumed grounding resistances with varying levels of accuracy are considered and the algorithm is used to obtain the actual resistances as shown in Fig. 6. The accuracy level of the assumed resistances are denoted by R_0 SNR in the figure and the noise level of the GIC measurements is 20 SNR for all the cases. The algorithm converges in fewer iterations when the assumed resistances are accurate, but the value it converges to is almost the same for all cases. This indicates that the estimation error is not sensitive to the accuracy of the assumed resistances, e.g. it is 9.3% when the assumed resistance has 509% error and 5.9% when the assumed resistances error is 11.2%.

The accuracy in the assumed resistance of individual substations have varying impact on the performance of the algorithm. To demonstrate this, one substation is taken for testing at a time; its assumed grounding resistance is set to have 200% error while all other substations have accurate assumed resistances. The SNR of the GIC measurements is 20 dB for all the cases and the E-field is assumed to be available to the algorithm. Fig. 7
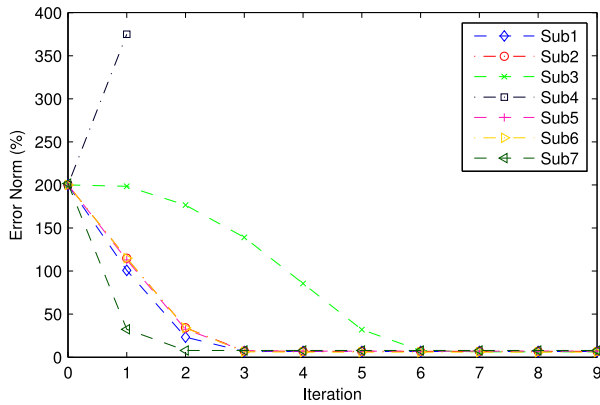
Fig. 7. The estimation error when different substations have inaccurate assumed resistances.
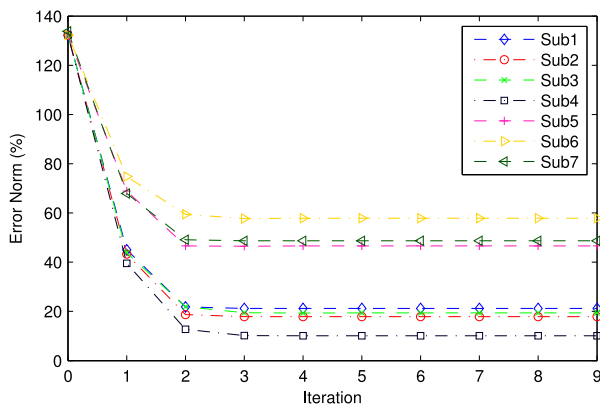

Fig. 8. The estimation error when different GIC sensors are subject to high level of noise.

illustrates the estimation error when different substations have inaccurate assumed resistances. It is observed that the algorithm is most sensitive to the accuracy of the assumed resistances at Sub 3 and Sub 4.

Next, the impact of the noise level of individual GIC sensors on the performance of the algorithm is analyzed. Gaussian noise with SNR equal to 20 dB is added to all the GIC sensors except for the one being tested, which has higher noise level with SNR equal to 5 dB. The estimation error when different GIC sensors are subjected to high level of noise is shown in Fig. 8. The assumed resistance of all the substations have 50% error and the E-field is known. The sensors at Sub 5, Sub 6 and sub7 are less robust to the measurement noise.

The error norm used so far for evaluating the estimation accuracy indicates the overall error of all the substations, but does not specify which substation contributes more to the total error. Fig. 9 illustrates the estimation error of individual substations when the GIC measurements have different levels of noise. All the assumed grounding resistances have 50% error and the E-field is known. It is observed that the estimation error at Sub 7 is the largest and contributes to most of the total error. The estimated resistance of other substations is quite accurate under all noise scenarios. This could relate to the structure of the
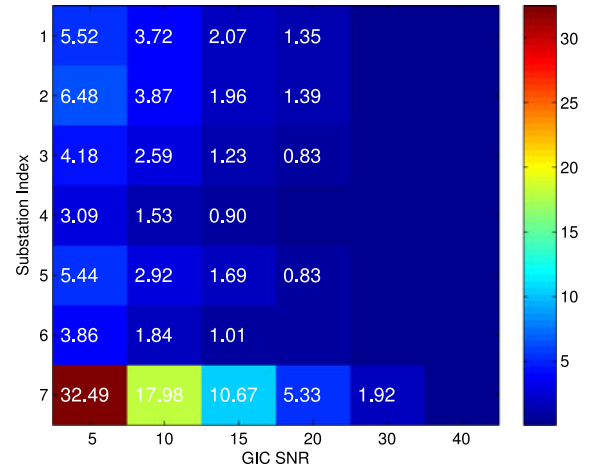

Fig. 9. The estimation error of individual substations when the GIC measurements have different levels of noise.

sensitivity matrices, $\mathbf{S}^N$ and $\mathbf{S}^E$ for this particular system. $\mathbf{S}^N$ and $\mathbf{S}^E$ both have very low values in their last column (row). This indicates that the GICs have low sensitivity to the grounding resistance of sub 7. Hence, the GIC measurements provide little observability to its resistance. The algorithm is generally not accurate in estimating the resistance of the substations with low sensitivities; However, it is still effective in improving the GIC calculation since such substations have low impact on the GICs regardless of their resistance values.

VI. APPLICATION OF THE RESISTANCE ESTIMATION ALGORITHM TO LARGER SYSTEMS

The algorithm is applied to a 62,500 bus, 27,600 substation model of the Eastern Interconnection used in [6]. The goal is to estimate the grounding resistance of the EI substations which are more critical to the GMD analysis and utilities might be more interested to find their values. High voltage transformers are more susceptible to GMDs and the existing GIC sensors already installed by utilities are often at such transformers. Motivated by this, the list of high voltage transformer in the EI system are considered. This includes more than 200 transformers with a high side voltage greater than 300 kV. Next, the top 100 transformers in the list which are most affected by GMDs are identified. This is done by calculating the GICs on the transformers under typical E-field profiles (northward and eastward field with unity magnitude) and selecting the ones which their average GICs are higher. A substation might have multiple transformers with high GICs in which case only one of the transformers are selected to avoid redundancy.

The same E-field data used for the 20-bus system is used here, i.e. the data for the March 9th, 2012 storm measured at Fredericksburg observatory. This E-field is enforced to the system and the induced GICs are calculated. White Gaussian noise with 30 dB SNR is added to the ideal GICs and the synthetic measurements are obtained.

The assumed grounding resistance of the 100 investigated substations are generated by adding noise with SNR equal to 10 to the actual resistances. Fig. 10 presents the actual and the
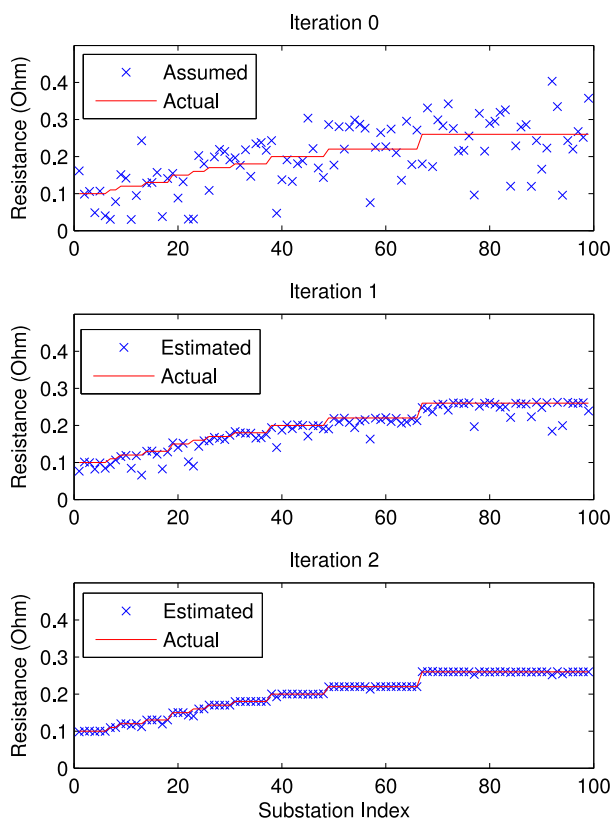
Fig. 10. The assumed, the estimated and the actual grounding resistances of the substations in the EI systems.

TABLE III
CORRELATION BETWEEN THE E-FIELDS ESTIMATED UNDER SUBSTATION
GROUNDING RESISTANCE UNCERTAINTY AND THE ACTUAL FIELD

Grounding Resistance Set	Northward E-Field		Eastward E-Field	
	Correlation	Norm Ratio	Correlation	Norm Ratio
R1	1.0000	0.79	1.0000	0.76
R2	1.0000	0.75	0.9997	0.82
R3	0.9999	0.77	0.9992	0.76
R4	0.9999	0.88	0.9998	0.90
R5	1.0000	0.86	0.9998	0.87

assumed resistances (iteration 0); the former is to be estimated by the algorithm and the latter is provided as the initial guess. Starting with the assumed resistances, the algorithm moves towards the actual resistances as shown in the figure (iteration 1 and 2). The E-field is assumed to be unknown for this experiment. The estimation error over the first iterations is calculated and it is observed that the error reduces from 120% to zero in three iterations.

Note that the actual resistances used for the EI system are fictitious and do not reflect the actual values of the real system. As was mentioned before, the grounding resistances are seldom available and so is the case for the EI system. The proposed algorithm can find the actual resistance of an EI substation, if its GIC measurement ever become available. On another note, the line and transformer resistances; and the network topology used in the study are obtained from the EI power flow model with good accuracy and the grounding resistance is the only piece of information which is missing in the model.

VII. CONCLUSION

In this paper, an analytical technique is developed which derives the substation grounding resistances from the GIC measurements. In this technique, the relation between the GICs and the grounding resistances is linearized through some sensitivity parameters and linear regression is used to solve for the resistances. The uncertainty in the grounding resistances introduces error to the parameters of the linear model. To tackle this, the problem is reformulated to decouple the uncertainties from the known parameters and regularized least squares is used for solving it. The effectiveness of the algorithm is evaluated using both a small test case as well as a 62,500 bus model of the EI system. As demonstrated, the algorithm can estimate the grounding resistances accurately even when the available GIC measurements are sparse and the assumed resistances have large error.

The paper suggests several directions for future research. First, the proposed algorithm should be applied to real GIC measurements as opposed to synthetic ones used here and its robustness to actual measurement noise and uncertainties needs to be validated. Second, the algorithm can be integrated into GIC model validation framework for improved performance. The grounding resistance uncertainty has been a challenge in GIC model validation framework and future research tend to address this issue by utilizing the proposed algorithm.

APPENDIX

This appendix demonstrates that the uncertainty in the substation grounding resistance affects the E-field estimation only by some scaling factor. Numerical results indicate that the sensitivity of the GIC at a particular substation to the grounding resistance of other substations is significantly lower than to its own grounding resistance. This implies that the sensitivity matrix is almost diagonal. Moreover, reference [11] demonstrates analytically that the sensitivity of the GIC at a substation to its grounding resistance does not depend on the E-field direction, i.e. the diagonal entries of the northward and eastward sensitivity matrices ($\mathbf{S}^N$ and $\mathbf{S}^E$) are equal. These two features of the sensitivity matrices (diagonally dominant matrices with approximately equal diagonal entries) suggests that the variation of the substation grounding resistances has linear impact on the E-field estimation.

Using the same setup as the one presented in the paper (Section VI), the E-field measured at Fredericksburg at March 9, 2012 is enforced to the EI system and the synthetic GIC data is generated for the 100 substations by solving the GIC power flow and obtaining the induced GICs. To model the worst case scenario, extremely inaccurate grounding resistances are considered with 510% error from the actual resistances. The E-field is estimated from the GIC data using LS method and the inaccurate grounding resistances. The estimated E-field is compared with the actual one and it is observed that the two fields have

extremely high correlation. This experiment is repeated for five different sets of assumed grounding resistances (termed as R1 to R5) with the same level of inaccuracy (around 500% error) and similar results are observed. Table III presents the Pearson correlation coefficient between the estimated E-field from each resistance set and the actual field and also the ratio of their Euclidean norms. The correlation is more than 0.999 even though the assumed resistances are extremely inaccurate. This verifies that the LS method estimates the E-filed accurately up to scaling in the presence of grounding resistance uncertainty.

REFERENCES

[1] North American Electric Reliability Corporation (NERC), "2012 special reliability assessment interim report: Effects of geomagnetic disturbances on the bulk power system," North Amer. Elect. Rel. Corp., Atlanta, GA, USA, Tech. Rep., Feb. 2012.

[2] V. D. Albertson, J. M. Thorson, R. E. Clayton, and S. C. Tripathy, "Solar-induced-currents in power systems: Cause and effects," *IEEE Trans. Power Appl. Syst.*, vol. PAS-92, no. 2, pp. 471–477, Mar. 1973.

[3] D. H. Boteler and R. J. Pirjola, "Modeling geomagnetically induced currents produced by realistic and uniform electric fields," *IEEE Trans. Power Del.*, vol. 13, no. 4, pp. 1303–1308, Oct. 1998.

[4] J. Kappenman, "Geomagnetic storms and their impacts on the U.S. power grid", Metatech Corp., Goleta, CA, USA, Tech. Rep. Meta-R-319, Jan. 2010.

[5] V. D. Albertson, J. G. Kappenman, N. Mohan, and G. A. Skarbakka, "Load-flow studies in the presence of geomagnetically-induced currents," *IEEE Trans. Power App. Syst.*, vol. PAS-100, no. 2, pp. 594–607, Feb. 1981.

[6] T. J. Overbye, T. R. Hutchins, K. Shetye, J. Weber, and S. Dahman, "Integration of geomagnetic disturbance modeling into the power flow: A methodology for large-scale system studies," in *Proc. North Amer. Power Symp.*, Sep. 2012, pp. 1–7.

[7] R. Horton, D. H. Boteler, T. J. Overbye, R. J. Pirjola, and R. Dugan, "A test case for the calculation of geomagnetically induced currents," *IEEE Trans. Power Del.*, vol. 27, no. 4, pp. 2368–2373, Oct. 2012.

[8] R. Pirjola, "Properties of matrices included in the calculation of geomagnetically induced currents (GICs) in power systems and introduction of a test model for GIC computation algorithms," *Earth Planets Space*, vol. 61, pp. 263–272, 2009.

[9] R. Pirjola, "Study of effects of changes of earthing resistances on geomagnetically induced currents in an electric power transmission system," *Radio Sci.*, vol. 43, 2008, Art. no. RS1004.

[10] K. Zheng *et al.*, "Effects of system characteristics on geomagnetically induced currents," *IEEE Trans. Power Del.*, vol. 29, no. 2, pp. 890–898, Apr. 2014.

[11] U. Bui, T. J. Overbye, K. Shetye, H. Zhu, and J. Weber, "Geomagnetically induced current sensitivity to assumed substation grounding resistance," in *Proc. North Amer. Power Symp.*, Sep. 2013.

[12] *IEEE Guide for Measuring Earth Resistivity, Ground Impedance, and Earth Surface Potentials of a Grounding System*, IEEE Std 81-2012, 2012 (Revision of IEEE Std 81-1983).

[13] A. P. S. Meliopoulos, G. Cokkinides, H. Abdallah, S. Duong, and S. Patel, "A PC based ground impedance measurement instrument," *IEEE Trans. Power Del.*, vol. 8, no. 3, pp. 1095–1106, Jul. 1993.

[14] F. Dawalibi and R. D. Mukhedkar, "Ground electrode resistance measurement in non-uniform soils," *IEEE Trans. Power App. Syst.*, vol. PAS-93, no. 1, pp. 109–115, Jan. 1974.

[15] G. F. Thug, *Earth Resistances*. London, U.K.: Georges Newnes Limited, 1964.

[16] F. Dawalibi and R. D. Mukhedkar, "Optimum design of substation grounding in two layer earth structure," Part I, Analytical Study, *IEEE Trans. Power App. Syst.*, vol. 94, no. 2, pp. 252–261, Mar. 1975.

[17] J. J. Leader, *Numerical Analysis and Scientific Computation*, Reading, MA, USA: Addison-Wesley, 2004.

[18] International real-time magnetic observatory network. [Online]. Available: http://www.intermagnet.org/

[19] R. A. Walling and A. N. Khan, "Characteristics of transformer exciting-current during geomagnetic disturbances," *IEEE Trans. Power Del.*, vol. 6, no. 4, pp. 1707–1714, Oct. 1991.

[20] O. H. Gish and W. J. Rooney, "Measurement of resistivity of large masses of undisturbed earth," *Terrestrial Magn. Atmospheric Elect.*, vol. 30, no. 4, pp. 161–188, 1925.

Maryam Kazerooni (S'11) received the B.S. and M.S. degrees both in electrical engineering from the Sharif University of Technology, Tehran, Iran, and the University of Windsor, Windsor, ON, Canada, in 2010 and 2012, respectively. She is currently working toward the Ph.D. degree in electrical engineering from the University of Illinois, Urbana-Champaign, Champaign, IL, USA. Her current research interests include power system reliability, state estimation, and geomagnetic disturbance analysis.

Hao Zhu (M'12) received the B.S. degree from Tsinghua University, Beijing, China, in 2006, and the M.Sc. and Ph.D. degrees from the University of Minnesota, Minneapolis, MN, USA, in 2009 and 2012, respectively. She is currently an Assistant Professor of ECE at University of Illinois, Urbana-Champaign, Champaign, IL, USA. Her current research interests include power system monitoring and operations, dynamics and stability, and energy data analytics.

Thomas J. Overbye (S'87–M'92–SM'96–F'05) was born in Milwaukee WI, USA. He received the B.S., M.S., and Ph.D. degrees in electrical engineering from the University of Wisconsin, Madison, WI, USA. He is currently the Fox Family Professor of electrical and computer engineering at the University of Illinois, Urbana- Champaign, Champaign, IL, USA. His current research interests include power system visualization, power system dynamics, power system cyber security, and power system geomagnetic disturbance analysis.